Thermodynamic and Voltammetric Characterization of the Metal Binding to the Prion Protein: Insights into pH Dependence and Redox Chemistry

Paul Davies,[‡] Frank Marken,[§] Simon Salter,[‡] and David R. Brown*[,‡]

Department of Biology and Biochemistry and Department of Chemistry, University of Bath, Bath BA2 7AY, U.K.

Received February 3, 2009

ABSTRACT: The prion protein is a high-affinity copper binding protein that plays a role in the neurodegenerative prion diseases when it is converted into an altered isoform. The function of the protein remains controversial, but its relationship to its metallochemistry has prompted further investigation. While many researchers continue to use short peptide models for binding studies, the clear discrepancy between data obtained with such models when compared to those of full-length recombinant proteins requires clarification with this more appropriate model. Isothermal titration calorimetry was used to assess metal affinity for PrP. Using both full-length native and recombinant prion protein, we have demonstrated that the prion protein binds copper but has little affinity for other metals. Metal binding is highly pH sensitive, being optimal at pH 7.5 for copper, nickel, and zinc and at pH 5.5 for iron. Metal binding affinity for PrP was not altered by protein glycosylation. The use of suitable thermodynamic modeling reveals complex and cooperative copper binding, with evidence of negative cooperativity within the octarepeat region. Cyclic voltammetry was utilized to assess the electrochemistry of copper-charged prion protein, and we show that mPrP has a redox potential of 0.03 ± 0.01 V versus the saturated calomel electrode at pH 7. The analysis also indicated that PrP is able to undergo reversible redox cycling with equal oxidative and reductive charges that are largely dependent on the copper bound to the octarepeat. The fifth site provides a small contribution to this redox activity, but only when the octarepeat is present. These results show conclusively that PrP can utilize copper for electron transfer, which would be expected for a radical detoxifying enzyme, and that the octarepeat region is the functional domain.

Prion diseases or transmissible spongiform encephalopathies are characterized by the conversion of a normal cellular glycoprotein, the prion protein (PrP^c),[1] into an abnormally folded, protease resistant isoform (PrP^{sc}) that is deposited in aggregates in specific areas of the central nervous system (*1*). These diseases include scrapie in sheep, bovine spongiform encephalopathy in cattle, and sporadic and variant Creutzfeld-Jakob disease in humans (*1, 2*). These diseases can occur in forms related to point mutations in the prion protein gene or be transmitted between individuals (*1, 3*). Regardless of the form of the disease, the prion protein is implicated in its pathology. Mice lacking expression of the prion protein cannot be infected with prion disease (*4*). The implication of this result is that PrP expression is essential for disease even if acquisition of the disease is dependent on challenge from an exogenous source of infectivity. For this reason, understanding the normal biology of the prion protein is essential to understanding the conversion mechanism that generates infectious prions.

The function of PrP^c continues to be debated. However, it is fairly well established that PrP^c is a cell surface protein that binds copper (*5*). Although a number of hypotheses concerning the function of the protein do not require the protein to bind copper, these studies are usually related to changes in cellular activity following manipulation of the protein rather than observation of the protein's activity. These activities include cell adhesion of cell signaling (*6*−*8*) and neurite outgrowth (*9*). The two main copper-dependent activities suggested for the protein are copper sequestration/internalization (*10*−*12*) and antioxidant/survival promoting factor (*13, 14*). Most proteins that bind copper offer some protection against copper's toxic effects. A significant body of data suggests that PrP^c is an antioxidant, possibly a superoxide dismutase (*5, 15*−*18*). However, further studies cast doubt on this theory (*19, 20*). With recent new data confirming the superoxide dismutase activity (*21, 22*), further investigation has become necessary.

PrP binds four to five atoms of copper at sites within an N-terminal octameric repeat region (*23*). The sites are centered around histidine residues within each repeat. The reported affinity of copper for full-length PrP is in the range that would bind nanomolar to picomolar concentrations of copper (*24*). However, studies with smaller fragments

* To whom correspondence should be addressed: Department of Biology and Biochemistry, University of Bath, Claverton Down, Bath BA2 7AY, United Kingdom. Phone: +44-1225-383133. Fax: +44-1225-386779. E-mail: bssdrb@bath.ac.uk.

‡ Department of Biology and Biochemistry.

§ Department of Chemistry.

[1] Abbreviations: ITC, isothermal titration calorimetry; PAGE, polyacrylamide gel electrophoresis; PCR, polymerase chain reaction; PrP, prion protein; PrP^c, cellular PrP; PrP^{sc}, scrapie isoform of PrP; PrP-null, recombinant mouse PrP with six histidines replaced with alanines; PrP-ΔOcta, recombinant mouse PrP with the four histidines in the octameric repeat region replaced with alanines; PrP-Δfifth, recombinant mouse PrP with the two histidines in the fifth copper binding site replaced with alanines; SCE, saturated calomel electrode; WT-PrP, wild-type recombinant mouse PrP.

10.1021/bi900170n CCC: $40.75
Published on Web 02/05/2009

produce more variable measures (*25, 26*). The coordination of metal appears to vary with the number of available octameric repeats and the number of copper atoms involved (*27*−*29*). It is also believed that positive cooperativity (*23, 30, 31*) plays a role in the binding, but there could also be negative cooperativity at high copper concentrations (*32*). Structural changes in the protein occur on binding of copper (*16, 33, 34*), but a clear picture of the structural changes and their importance to PrP function remain unknown.

Despite considerable study of the copper binding capacity of PrP^c, many unresolved issues remain. Many studies on copper binding to PrP have been based on peptides (*25, 26, 33, 35*), but comparison to studies of full-length recombinant PrP suggested that many of these studies are unreliable (*24*). In particular, it remains unclear whether the so-called fifth copper binding site plays a major role in copper binding. Other issues that have not been assessed fully include the pH dependence of the individual sites, which metals besides copper bind to PrP, and the electrochemical properties of the copper once bound to the protein. Furthermore, despite suggestions that copper binds to native PrP extracted from mouse brain (*5*), the affinity of copper for native, glycosylated PrP has not been determined. In this work, we explore all these issues and demonstrate that glycosylation does not alter the affinity of copper for PrP, several other divalent transition metals bind PrP, the fifth site binds copper with only high affinity, and PrP can effectively channel electrons when copper is bound. These data indicate that PrP binds copper effectively in the physiological range and has the electrochemical properties characteristic of its previously suggested function as a superoxide dismutase. Previous reports of cooperativity within the octameric region are also investigated and confirmed in real time.

MATERIALS AND METHODS

Recombinant Protein Production. Recombinant mouse PrP protein was produced as described previously (*24*). All proteins used for this study were not tagged. Briefly, PCR-amplified product was cloned in expression vector pET-23 (Novagen) and transformed into an *Escherichia coli* ad494(DE3) or BL21(DE3) strain. Expressed proteins were solubilized by sonication in 8 M urea and recovered by immobilized metal ion affinity chromatography (IMAC). Columns were charged with copper. The eluted material was treated with 0.5 mM EDTA to ensure the protein was free from metal ions potentially leached from the IMAC column. Additionally, all subsequent treatments were performed with doubly deionized water treated with Chelex resin, (Sigma) to remove residual metal ions. The denatured protein was refolded by a 10-fold dilution of the urea in deionized water followed by concentration by ultrafiltration and two rounds of dialysis to remove residual urea, imidazole, and EDTA. Starting stock solution protein concentrations were measured using theoretical extinction coefficients at 280 nm (http://us.expasy.org/tools/protparam.html) and confirmed by a Bradford assay (Sigma). The final protein was concentrated or diluted to 20 μM in Chelex-treated water adjusted to the appropriate pH by addition of a concentrated buffer stock (final concentrations of 10 mM MES for pH 5.5−7, 10 mM sodium acetate for pH 4−5.5, or 10 mM MOPS for pH 7−9). Protein purity was checked using polyacrylamide gel electrophoresis under denaturing conditions stained with Coomassie brilliant blue.

Proteins used in this study included WT-PrP (wild-type mouse PrP, residues 23−231); PrP-Δfifth, a mutant lacking the fifth copper binding site (WT-PrP but with H95A and H110A mutations); PrP-ΔOcta, a mutant with the histidines of the octameric repeat replaced with alanine residues (i.e., WT-PrP but with H60A, H68A, H76A, and H84A mutations); and PrP-null, a mutant lacking all six N-terminal histidines (i.e., WT-PrP but with H60A, H68A, H76A, H84A, H95A, and H110A mutations).

Mutagenesis. Constructs expressing mPrP amino acids 23−231 of untagged mouse PrP and the PrP-Δfifth mutant were prepared as previously described (*24*). The PrP-null mutant and the PrP-ΔOcta mutant were prepared by mutagenesis of the first two constructs to replace the four histidine residues of the octameric repeat region with alanine residues. Overlapping splint oligonucleotides were used for each site. Four successive rounds of mutagenesis were used to mutate each of the four histidines sequentially. Each round of mutagenesis was confirmed by DNA sequencing. Successful mutations of all four histidines resulted in the generation of PrP-null from PrP-Δfifth and PrP-ΔOcta from WT-PRP.

The following oligonucleotide sequences were used (forward primers only): H60A, 5′-GGG GCA GCC CGC CGG TGG TGG CTG-3′; H68A, 5′-GGG ACA ACC CGC TGG GGG CAG CTG G-3′; H76A, 5′-GGG GAC AAC CTG CTG GTG GTA GTT GGG G-3′; and H84A, 5′-GGG TCA GCC CGC TGG CGG TGG ATG-3′. Reverse primers were complementary to the forward primers.

Isolation of Native PrP. Brains of adult mice (MF1) were collected and sonicated in lysis buffer [50 mM Tris, 100 mM NaCl, and 20 mM EDTA (pH 7)]. Ten brains were prepared in 100 mL of lysis buffer. The solution was left to stand on ice for 30 min and then centrifuged at 14K rpm The pellet was collected and washed three times in a buffer containing 0.1 M Tris (pH 7). After the third wash, the pellet was dissolved in a buffer containing 8 M urea, 50 mM Tris, and 100 mM NaCl (pH 7). The dissolved pellet was filtered through a 0.45 μm filter before being applied to an IMAC column. The IMAC column was charged with copper. The protein extract was applied to the column and washed with wash buffer [8 M urea, 50 mM Tris, and 100 mM NaCl (pH 7)]. After approximately 10 bed volumes, the buffer was changed to wash buffer with 20 mM imidazole. After being extensively washed (at least 50 bed volumes), the bound protein was eluted with wash buffer containing 120 mM imidazole. The purity of the protein was ascertained using a Coomassie-stained PAGE gel and Western blotting with a PrP specific antibody (DR1).

Isothermal Titration Calorimetry Measurements. ITC experiments were carried out on a Microcal VP-ITC. A series of injections of metal were made into an isolated chamber containing the protein at a constant temperature of 25 °C. Heat changes within the cell were monitored during each injection of metal and recorded as the total heat change per second over time. A binding isotherm was then fitted to data and expressed as the heat change per mole of metal against the metal to protein ratio. From this data, a model is used to predict the number of binding sites on the protein involved

in the reaction, the association constants of the binding (K_a), and the change in enthalpy (ΔH).

Protein samples were prepared by adding a small amount of concentrated and pH-adjusted buffer as before to a final concentration of 10 mM buffer and either 10, 12, 15, or 20 μM protein. Different concentrations were used to ensure that results were repeatable over a variety of conditions. The choice of buffers was based on initial trials, which revealed that these buffers offered the minimum of background noise.

The use of free copper in the titrations results in protein aggregation and nonspecific binding (*36*). ITC binding experiments involving tight binding models in which the affinity for the ligand is likely to exceed 10^9 M^{-1} require the use of a weaker chelator to accurately determine dissociation constants (*37, 38*). In addition, no free copper exists in vivo so a copper chelate was used. Copper solutions were prepared by adding copper sulfate to 10 mM buffer (as above) along with glycine in a molar ratio of 1:4. Glycine chelates two molecules of copper, forming a $Cu(gly)_2$ complex. The excess glycine thus ensures that there is never any free copper in the reaction cell, avoiding the complications mentioned above. Buffer was added to the metal to ensure that the strong acidity of copper sulfate did not overwhelm the buffering capacity of the protein solution. Titrations of copper sulfate (30×4 μL) into an unbuffered protein solution show a total change of -1 pH unit (data not shown). The use of buffer in only one of the solutions would result in significant background noise; therefore, both protein and metal solutions were buffered. The concentration of copper used was dependent on the concentration of protein in the reaction cell. The final ratio of protein to copper in the reaction cell after each ITC experiment was 1:10.

During each experiment, 30×4 μL doses of copper were injected into the chamber of protein, which was stirred constantly at 300 rpm. Each injection was followed by a 2 min period to ensure equilibration of the solution. All experiments were repeated three times and where possible using different concentrations of separately prepared protein. Data were analyzed using Origin 5.0 with the Microcal software patch installed. Each experimental condition had a blank run with protein in the chamber replaced with buffer. These data were then subtracted from the run with protein present to take into account any energy of dilution or metal/buffer reaction. A binding isotherm was then fitted to the data using a least-squares calculation to yield a χ^2 value. The isotherm that fitted with the lowest χ^2 was taken as a best-fit model. From this model, values for K_a and ΔH were calculated along with the most likely number of binding sites involved. The K_a values were then adjusted to factor in the affinity of copper for glycine. Previous studies have shown glycine to bind two atoms of copper with the following affinities: $K_1 = 4.0 \times 10^5$ M^{-1} and $K_2 = 1.7 \times 10^4$ M^{-1} with $\beta_2 = 6.8 \times 10^9$ M^{-1} at pH 7 (*39*). These values also vary with pH. The relative contribution of each of these species at the prevalent pH was then used in the final equilibrium to fully account for the effect of the chelate, as previously reported (*40*). In addition, sequential modeling was carried out on data obtained from constructs at pH 7 and 8. For these models, final values were adjusted as previously shown (*41*).

ITC experiments with other metals were carried out using the same procedure except glycine was not used.

Cyclic Voltammetry. Voltammetric measurements were conducted with a μ-Autolab III potentiostat system (Eco Chemie) in a conventional three-electrode electrochemical cell. Experiments were performed in staircase voltammetry mode (step potential of 0.6 mV) with a platinum gauze counter and a saturated calomel reference electrode (SCE, REF401, Radiometer). The working electrodes used were 5 mm diameter edge plane pyrolytic graphite (Pyrocarbon, Le Carbon) or 3 mm diameter boron-doped diamond (Diafilm, Windsor Scientific) electrodes. Electrodes were polished on fresh micro cloths (Buehler) with alumina (1 μm, Buehler) as a polishing aid. After the final polish on a clean micro cloth, electrodes were rinsed with demineralized water. Aqueous solutions were thoroughly deaerated with argon (BOC) before data were recorded. All measurements were taken at 22 ± 2 °C. Voltammetric measurements were conducted in an aqueous buffer solution (5 mM MES/Tris at pH 7) thoroughly deaerated with argon. The working electrode was polished and the background current recorded in the absence of protein. Next, the working electrode was immersed in a protein solution (containing 20 μM recombinant mPrP in buffer) and after 60 s removed and rinsed with water. A longer incubation did not significantly increase the amount of immobilized protein. The resulting protein-modified electrode was reimmersed in the pure buffer solution in the measurement cell, and cyclic voltammograms were recorded. Adhesion of protein to the edge plane pyrolytic graphite and to the boron-doped diamond electrode surfaces was excellent, and stable signals were obtained for many potential cycles.

RESULTS

pH Sensitivity of Copper Binding to Recombinant PrP. A thorough study of copper affinity across the full pH range has not been carried out on full-length PrP. To overcome copper solubility issues within this pH range, and to minimize potential oxidative effects from free copper, we used a chelator to deliver metal to the protein. The effect of this chelator was then fully included in the overall equilibrium (*40*), using the enthalpy- and pH-adjusted literature values (*39*). The metal chelate was titrated through each experiment to reach a 10-fold molar ratio excess by the end. As a control, PrP-null was used. This mutant lacks all six histidine residues of the N-terminal domain of PrP. The titration of copper into the ITC reaction cell containing WT-PrP resulted in a net release of heat. For PrP-null, no reaction over the energy of dilution was detectable. Figure 1 shows examples of the ITC traces obtained for WT-PrP and PrP-null at pH 7.

The copper binding sites of PrP consist of the octameric repeat region and the so-called fifth site. The octameric region has been reported to contain four binding sites each consisting of an octameric repeat for which copper binding is largely dependent on a histidine of each segment (*25, 42*). The fifth site consists of a region containing two histidines distal to the octameric repeat. Two mutants, PrP-Δfifth and PrP-ΔOcta, were used to assess the pH dependence of copper binding at these two sites. Although the histidines suspected to be responsible for copper coordination have been replaced with alanine to abolish binding, the peptides are still full-length for the study of the effects within the intact protein as opposed to peptide fragments, the results from which may

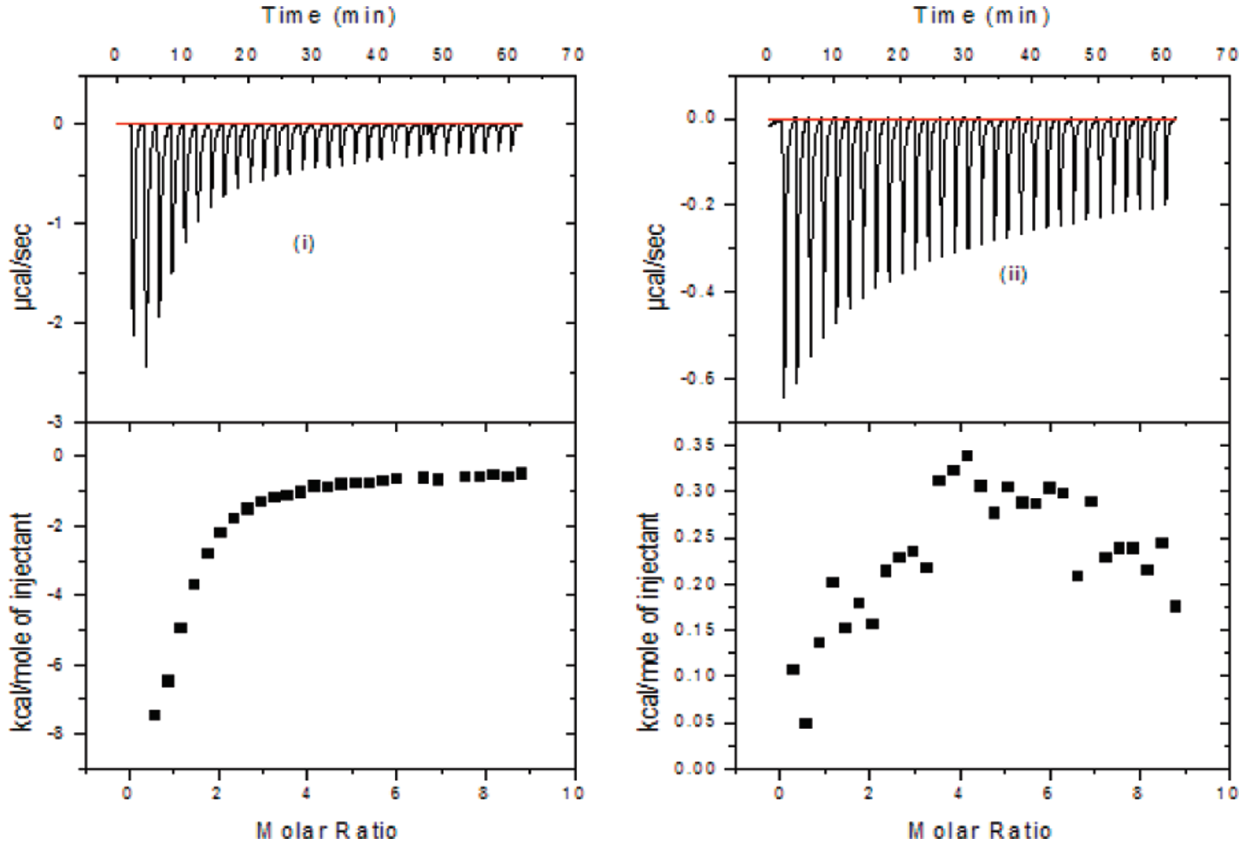

FIGURE 1: Examples of ITC experiments with WT-PrP at pH 7.5 and 4. Traces from the titrations of 2 mM $CuSO_4$: 8 mM glycine in 10 mM Mes (pH 7) (i) into 20 μM WT-PrP and 8 mM glycine in 10 mM Mes (pH 7) (ii) into 20 μM PrP-null. The negative peaks seen on the traces are representative of a net release of energy from the system during each injection of copper. The top trace in each case shows the raw data, plotted against time, while the bottom trace shows the data corrected for the energy of dilution and buffer interactions. These data are plotted as the energy lost per mole of copper against the ratio of copper to protein. From this bottom trace, a model can be applied to fit the most likely number of binding sites and their affinity for the copper. The line running through the data points on the trace represents this model's best line of fit. Both one and two sets of independent site regression models were used for fitting data to enthalpy and affinity values. In each case, the model that provided the most sensible fit in terms of χ^2 and stoichiometry was used. For all cases, a two sets of sets model provided the best fit, with the exception of PrP-ΔOcta at pH 5 and PrP-Δfifth at pH 5, 6, and 9, where a single set of sites model was more appropriate. The mean values obtained from three independent experiments are presented in Tables 1−3. The number of sites present varied with pH. No copper binding was detected below pH 5. For the wild-type protein under acidic conditions, two sets of sites are clearly distinguished, with log stability constants increasing from 4.3 and 5.1 at pH 5 to 6.3 and 6.9, respectively, at pH 5.5. At pH 6, a second site appears within the second group of binding events, with stability constants for the two sets of sites of 8.4 and 6.1. Optimal copper binding occurs from pH 7 to 7.5 with a single high-affinity site, with a log stabililty constant of 10.8 at pH 7.5, and then four related sites, with a log stability constant of 7.3. After this point, the number of sites and their affinity for copper decrease.

Table 1: Log Stability Constants and Number of Sites for Copper on Wild-Type PrP across the pH Range As Determined by ITC Using a Two-Independent Site Model[a]

pH	n_1	log K_1	n_2	log K_2
4	not determined	−	not determined	−
5	1.019 ± 0.084	4.3	1.000 ± 0.000	5.1
5.5	1.008 ± 0.012	6.3	1.031 ± 0.051	6.9
6	1.021 ± 0.026	8.4	1.985 ± 0.249	6.1
6.5	1.017 ± 0.051	9.2	3.741 ± 0.219	6.5
7	1.092 ± 0.116	10.2	4.031 ± 0.102	6.9
7.5	0.946 ± 0.037	10.8	4.048 ± 0.897	7.3
8	1.058 ± 0.123	10.4	4.007 ± 0.195	7.0
9	1.142 ± 0.083	9.6	2.091 ± 0.281	6.4

[a] n_1 and n_2 represent the number of sites detected within each group of sites. The total number of binding events is therefore equal to $n_1 + n_2$. Log K values have been adjusted to account for the relative contribution of the chelator species to the overall equilibrium at the relevant pH at 25 °C. The means of three independent experiments were calculated, with errors between K values not exceeding 5%.

Table 2: Log Stability Constants and Number of Sites for Copper Binding to PrP-Δfifth across the pH Range As Determined by ITC Using a One- or Two-Independent Site Model[a]

pH	n_1	log K_1	n_2	log K_2
4	not determined	−	not determined	−
5	1.026 ± 0.162	5.2	not determined	−
6	1.061 ± 0.009	8.7	2.001 ± 0.052	5.8
7	1.198 ± 0.043	10.5	2.896 ± 0.376	6.4
8	1.062 ± 0.101	10.1	2.961 ± 0.061	6.1
9	1.035 ± 0.109	9.0	1.117 ± 0.151	7.4

[a] n_1 and n_2 represent the number of sites detected within each group of sites. The total number of binding events is therefore equal to $n_1 + n_2$. Log K values have been adjusted to account for the relative contribution of the chelator species to the overall equilibrium at the relevant pH at 25 °C. The means of three independent experiments were calculated, with errors between K values not exceeding 5%.

not fully represent the true copper chemistry of PrP. By comparing these two constructs with wild-type PrP, we should be able to distinguish the relative contribution of each region on PrP to the overall copper binding seen on the wild-type protein. Figure 2 shows a comparison between the isotherms from the wild type, the Δfifth site, and the octarepeat. The acuteness of the slope is indicative of the overall and combined affinity of the ligand for the metal. The fifth site, when examined in isolation, produces an isotherm indicative of high-affinity binding, as demonstrated

Table 3: Log Stability Constants and Number of Sites for Copper Binding to PrP-ΔOcta across the pH Range As Determined by ITC Using a One- or Two-Independent Site Model[a]

pH	n_1	log K_1	n_2	log K_2
4	not determined	−	not determined	−
5	1.096 ± 0.140	4.4	not determined	−
6	1.047 ± 0.066	8.5	not determined	−
7	0.962 ± 0.030	10.5	1.057 ± 0.018	6.1
8	1.019 ± 0.092	10.3	1.104 ± 0.131	6.1
9	1.301 ± 0.251	9.3	not determined	−

[a] n_1 and n_2 represent the number of sites detected within each group of sites. The total number of binding events is therefore equal to $n_1 + n_2$. Log K values have been adjusted to account for the relative contribution of the chelator species to the overall equilibrium at the relevant pH at 25 °C. The means of three independent experiments were calculated, with errors between K values not exceeding 5%.

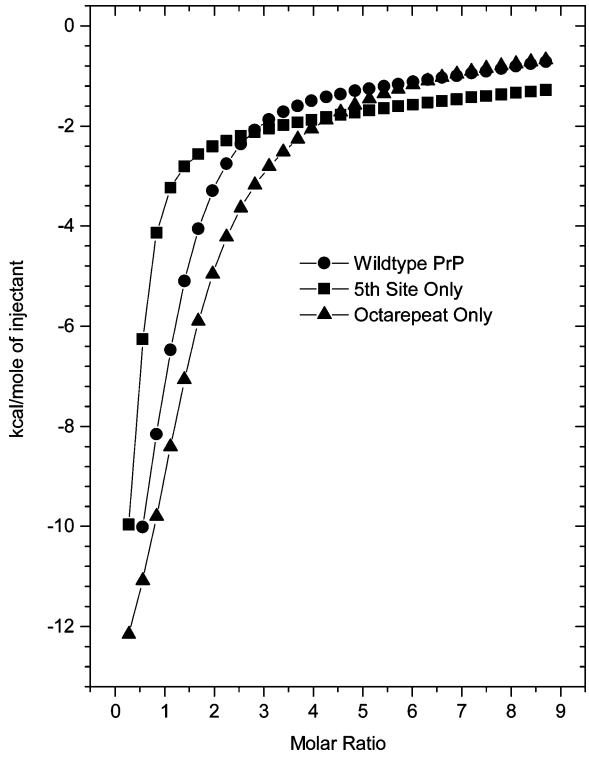

FIGURE 2: Comparison of isotherms obtained for copper binding to wild-type PrP, PrP-Δfifth, and PrP-ΔOcta. In all cases, 2 mM $CuSO_4$ with 8 mM glycine in 10 mM MES (pH 7) was titrated into 20 μM protein with 8 mM glycine in 10 mM MES (pH 7). The steepness of the curve is representative of the degree of binding tightness. A clear difference can be seen between the three conditions during the initial three ratios of titrated copper. The fifth site when in isolation binds copper with a higher affinity than the octarepeat region, and the wild-type protein displays an intermediate pattern of stability between the two.

by the steep initial slope and rapid transition to a plateau at saturation. The octarepeat region shows an initial steep slope followed by a slow transition to the saturation plateau, indicative of high-affinity binding followed by lower-affinity, multiple binding events. The wild-type protein, as expected, is approximately between the slopes.

Tables 2 and 3 show the data for the octarepeat and fifth site region, respectively. At pH 5, the octarepeat region binds only one copper, with an affinity almost identical to that of the second site seen on the wild-type protein. The first site on wild-type PrP can be matched to the site apparent on the fifth site region at this pH. As the pH increases, the first binding event apparent on the wild type closely matches the high-affinity site seen in the fifth site region. However, at pH 7 and 8, a second low-affinity site, with a log stability constant of 6.1, appears which is not reflected in the matched fifth site on the wild-type protein. Additionally, when examined in isolation, the octarepeat region appears to bind copper with complexity greater than that first indicated by the wild-type data. Two sets of sites are detectable on the octarepeat region at pH >5, with a high-affinity binding event followed by a lower-affinity event. At pH 7, the lower-affinity events increase to three, with the single site increasing to a log stability constant of 10.5. As with the wild-type protein, the number of sites and their affinity decrease under more basic conditions from pH 8.

Table 4: Log Stability Constants and Number of Sites for Copper Binding to Three PrP Constructs across the pH Range As Determined by ITC Using a Sequential Site Model[a]

construct	log K_1	log K_2	log K_3	log K_4	log K_5
wild-type	10.4	10.1	5.9	6.9	7.1
Δfifth site	10.6	6.1	not determined	not determined	not determined
Δoctarepeat	10.5	6.0	7.0	7.0	not determined
native PrP^c	10.0	9.9	6.1	6.9	6.9

[a] Log K values have been adjusted to account for the relative contribution of the chelator species to the overall equilibrium at the relevant pH at 25 °C. The means of three independent experiments were calculated, with errors between K values not exceeding 5%.

Previous reports have suggested a cooperative binding mechanism exists within the octarepeat region for copper (*32*). Deriving values for such a binding mechanism is possible with ITC, but where sites within a group of sites are nonidentical, it leads to a degeneracy within the ITC two-site model (*40*). Under such circumstances, it is appropriate to analyze such data using a thermodynamic model that assumes that sites are filled sequentially and each site is affected by the previous binding event. This can then yield important details concerning each individual binding event within a group of sequentially filled sites. Such a model exists within Origin supplied by Microcal but makes the factoring of the chelator effect to the overall equilibrium complicated and potentially error prone. We have previously demonstrated the feasibility of this model (*41*) and can now apply it to the data from wild-type PrP and the two mutants. Table 4 presents the data from the wild-type, octarepeat, and fifth site constructs analyzed by a sequential binding model. In comparing the affinity constants of the three proteins, we can see similarities between the first two binding events on the wild-type protein and the first event on the two mutants. The next three wild-type binding events closely match the pattern and affinity of the last three events on the octarepeat construct. This suggests that there are two high-affinity sites on the wild-type protein, one within the octarepeat region and one within the fifth site. It cannot be totally ruled out that the octarepeat region binds only three copper ions and the fifth site two copper ions at pH 7. However, the affinity values for copper and the octarepeat region do more closely match the last four events on the wild-type protein.

Copper Affinity of Native PrP. It is clearly important to identify whether the findings from the recombinant protein are at all relevant to the cellular form (PrP^c). Isolation of PrP^c from mouse brain or culture mouse neurons demonstrated that copper binds to native PrP. However, the affinity

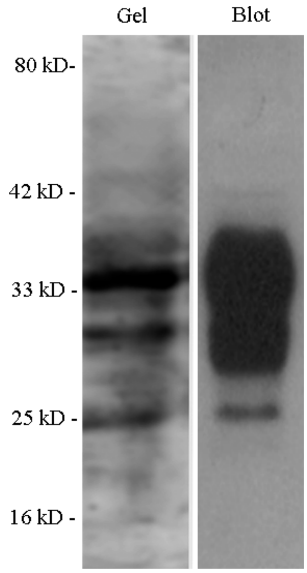

FIGURE 3: Purification of native PrP. Native mouse PrP was purified from the brains of adult mice. The purity was assessed by electrophoresis on a PAGE gel and staining with Coomassie blue (gel). The presence of PrP was verified using Western blotting and immunodetection with a specific antibody (blot). Native PrP has three glycoforms as indicated by the presence of three strong bands. The nongycosylated form is 25 kDa with the heavy diglycosylated form at around 33 kDa. Monoglyosylated PrP is intermediate between the two and can be represented by either one or two bands.

of copper for native PrP has not been determined. To do this, it is necessary to purify PrP^c from the brain and strip any bound copper from it before carrying out ITC experiments. A novel isolation technique was developed. In the first step, membranes were isolated from adult mouse brains. The membranes were then exposed to EDTA to remove bound copper. After dialysis, the membranes were solubilized with detergents and applied to a copper-charged IMAC column. The eluted protein was analyzed by gel electrophoresis and Western blotting. The only bands observed on a silver-stained gel were those that corresponded to PrP bands in a Western blot (Figure 3). The purified protein was then used for ITC experiments at pH 7.4 and 5.5. The values obtained were very similar to values for recombinant mouse PrP, compared in Table 4. This suggests that native PrP has the same affinity for copper as recombinant PrP, and this affinity is not affected by glycosylation.

Affinity of PrP for Other Metals. There have been numerous suggestions that PrP can bind other metals such as nickel, zinc, and iron. As these can be found in a free ionic form and do not necessarily form complexes with glycine, ITC experiments were carried out to assess the affinity of ionic zinc, iron, and magnesium for recombinant mouse WT-PrP in the absence of glycine. Table 5 lists the values obtained at (i) pH 5.5 and (ii) pH 7. At pH 7, mPrP bound all the divalent cat ions tested at two sites with the exception of magnesium, which did not bind. Zinc, nickel, and iron all displayed similar affinities in the first site with zinc and nickel similar at the second site, suggesting the protein is able to bind these metals in the micromolar range. The second iron site displayed affinities in the millimolar range. When metal binding was analyzed in the mPrP mutant lacking the fifth site or the octarepeat, it was found that both nickel and zinc bound at two sites within the octarepeat with affinities matching those in the wild-type protein. Interestingly, it was also found that protein with only the fifth site also had a low-affinity site for zinc that was not apparent in the wild type. In contrast, iron seems to bind with highest affinity within the fifth site with the second low-affinity site seen in the wild type appearing in the octarepeat region. At pH 5.5, only iron exhibited binding, and that appeared to be at the micromolar affinity site within the fifth site region.

Electrochemical Analysis. Voltammetric experiments were conducted in aqueous solution containing 5 mM Mes/tris buffer at pH 7 and no dissolved protein. Refolded mPrP proteins are known to strongly bind to surfaces, e.g., mineral surfaces (*43*), and this effect is very beneficial for voltammetric studies. Adsorption of the copper-refolded protein onto edge plane pyrolytic graphite or boron-doped diamond electrode was readily achieved, and highly reproducible reversible current responses were obtained. Due to considerably lower capacitive background current at boron-doped diamond electrodes, these were chosen for further examination. Figure 4ii shows a typical cyclic voltammogram obtained with a scan rate of 10 mV s^{-1}. The background current (see the dashed line) at this electrode is clearly different, and the reduction and reoxidation processes can be assigned to the copper centers in copper-refolded Cu-mPrP. Experiments with pure mPrP protein in the absence of copper did not show this signal.

To examine this redox process in more detail, we examined the effect of scan rate. Panels i−iii of Figure 4 show a typical sequence of voltammetric data, and the plot in panel iv of Figure 4 clearly demonstrates a linear relationship between peak current and scan rate. This confirms a permanently surface bound protein and electron transfer directly into the protein-bound copper. The effect of the scan rate on the peak potentials is shown in Figure 4v. The characteristic logarithmic dependence is consistent with an electron transfer rate-limited process, and a fit of the corresponding equation for the peak potential (*44*) gives good agreement with an α of 0.5 and a k^0 of 0.05 s^{-1}.

$$E_p = E_{mid} + \frac{RT}{\alpha F} \ln\left(\frac{RT}{\alpha F}\frac{k^0}{\upsilon}\right) \quad (1)$$

where the peak potential (E_p) is correlated to the midpoint potential (E_{mid}), the gas constant (R), the absolute temperature (T), the transfer coefficient (α), the Faraday constant (F), the standard rate constant for electron transfer (k^0), and the scan rate (υ).

The copper-bound protein contains five copper centers, four localized relatively closely together in the octarepeat unit and one within the so-called fifth site. The charge under the voltammetric response, ca. 255 nC, can be investigated and converted into the approximate area per protein adsorbed onto the boron-doped diamond surface. This calculation gives a very realistic area of 4.7 nm × 4.7 nm for each Cu-mPrP molecule (molecular mass of 23 kDa), assuming that five copper centers are reduced in one-electron processes (five electrons consumed per protein). These five copper centers may be electronically distinct but coupled and therefore may not be individually resolved. The reversible or midpoint potential for this process is 0.03 ± 0.01 V versus SCE, which is not too different when compared to the reversible potential observed for Cu(II/I) coordinated to fragments of the prion protein (*45, 46*).

Table 5: Log Stability Constants and Number of Sites for Other Divalent Cations Binding to Three PrP Constructs As Determined by ITC[a]

	wild type		no fifth site		fifth site only	
	site 1	site 2	site 1	site 2	site 1	site 2
			(i) pH 5.5			
Ni^{2+}	not determined	not determined	not determined	not determined	not determined	not determined
Zn^{2+}	not determined	not determined	not determined	not determined	not determined	not determined
Fe^{2+}	3.1	not determined	not determined	not determined	3.3	not determined
Mg^{2+}	not determined	not determined	not determined	n/dnot determined	not determined	not determined
			(ii) pH 7			
Ni^{2+}	4.3	3.2	4.4	3.2	not determined	not determined
Zn^{2+}	4.6	3.7	4.6	3.4	2.4	not determined
Fe^{2+}	4.0	2.7	2.8	not determined	3.9	not determined
Mg^{2+}	not determined	not determined	not determined	not determined	not determined	not determined

[a] Values quoted are log *K* stability constants derived from either one- or two-independent site models. All experiments were conducted in triplicate using buffers and concentrations previously described at 25 °C.

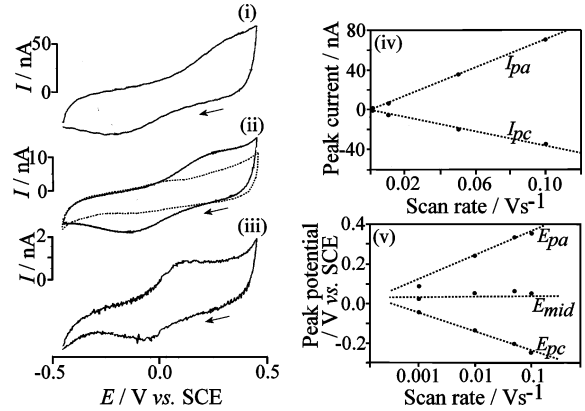

FIGURE 4: Representative cyclic voltammograms of WT-PrP bound to copper. Cyclic voltammograms recorded at scan rates of (i) 50, (ii) 10, and (iii) 1 mV s^{-1} for the reduction and reoxidation of copper-refolded mPrP adsorbed onto a 3 mm diameter boron-doped diamond disk electrode and immersed in 5 mM Mes/tris buffer solution at pH 7. The dashed line indicates the background signal without protein. (iv) Plot of the peak current vs the scan rate. (v) Plot of the peak potentials vs the scan rate (in logarithmic scale).

Table 6: Comparison of the Integrated Peak Charges (forward reaction) from WT-PrP, PrP-Δfifth, PrP-ΔOctaHis, and PrP-null-His As Obtained from Cyclic Voltammetry

protein	midpoint potential (V vs SCE)	integrated oxidation peak charge (nC)
wild-type mPrP-Cu	0.03	255
mPrP-Cu with no fifth site	0.03	201
mPrP-Cu with no octarepeat	−0.02	13
mPrP-Cu-null histidine	not available	not detected

To explore the dependence on copper for the protein's apparent redox chemistry, we conducted further experiments on mutant constructs of mPrP lacking either all the histidines in the octarepeat region (PrP-ΔOcta), the fifth site (PrP-Δfifth), and both the fifth and octarepeat (PrP-null). The integrated peak current for each of these proteins is compared with that of wild-type mPrP in Table 6. As expected, the null-His protein produced no significant oxidation or reduction peak. The other three proteins all produced fully reversible redox signals, with the wild-type protein producing the largest. When five atoms of copper are bound to the protein (four in the octarepeat and one at the fifth site), an integrated charge of 255 nC can be calculated from the forward reaction. When copper binding at the fifth site is abolished, a drop equivalent to 20% is observed. When copper binding in the octarepeat is nullified, however, a 95% decrease in charge is observed. This suggests that electron transfer at the fifth site is facilitated by the coppers present within the octarepeat, and it is these coppers that are responsible for the protein's apparent ability to cycle electrons when adsorbed to an electrode system.

DISCUSSION

There has been a long and somewhat inconsistent line of publications on the relationship between PrP and copper (*16*, *23*−*34*). Such an enormous variation in opinion on what is fundamental knowledge for a metalloprotein deserves and demands an explanation and re-examination. We present here a thorough thermodynamic and spectroscopic study of copper binding to recombinant PrP and, through use of single-amino acid changes, demonstrate the contribution of each binding site in the wild-type protein to the overall copper binding equilibrium.

The key aspects of the protein still under debate are its function and the role of metal binding in its physiological role and in disease. These questions are difficult to answer when reports of the protein's affinity for copper range from micromolar (*47*) to femtomolar (*26*). Although it is almost universally accepted that the protein binds copper (*5*) and more recently binds copper in a complex and cooperative way (*28*), some aspects of the metal−protein complex require further clarification. Among these unknowns are the pH dependence of metal binding, what other metals bind and where, and what implications on the function of the protein these associations have. Although there has been much work focused on the individual binding regions of the protein by use of peptide fragments, there are few data on how the individual regions behave when in the intact protein. In addition, most studies have centered on the recombinant protein, and therefore, the effects of in vivo processes, such as glycosylation, have yet to be considered. This study uses the complete protein to study these individual metal binding regions and provides a thorough insight into its metallochemistry and its relevance in the native protein.

To explore the effect of pH on copper binding to the prion protein, we employed isothermal titration calorimetry to predict the number of sites and their affinity for the copper ion across a range of pH from 4 to 9. The affinities, stoichiometries, and degrees of cooperativity we report here are in very close agreement with those from a previous study

(*48*). The protein's optimal binding is between pH 7 and 7.5, which would mean that in vivo conditions of pH 7.4 would favor a tight copper association. We have demonstrated that both the octameric repeat and the fifth site of wild-type PrP can bind copper with high affinity. The two copper sites within the fifth site highlighted by other studies using peptides (*49*) do not appear to be present in the complete protein. It seems that, in the presence of the octarepeat region, the fifth site binds a single copper, pointing toward a repressive effect by the octarepeat region. The combined affinity of the two sites with the fifth binding region identified by this and other studies of log 16.7 would appear to be reduced to a single binding event of around log 10.4 in the wild-type construct. The octarepeat region binds four coppers in both the wild-type protein and the protein with the fifth site silenced at physiological pH. This study has demonstrated the different binding modes of the octarepeat reported in previous studies (*28*) by studying copper binding at different pHs. Under acidic conditions between pH 5 and 6, strong competition from protons for the glycine amides, pI 9.63 (*39*), means that only the imidazoles from the four histidines, pI 6.03 (*39*), are available for copper coordination. This results in a single complex involving one copper ion binding to four histidine imidazoles, irrespective of the copper concentration. As the pH increases to 6, the four imidazole complexes split to bind one copper to two imidazoles, representing an intermediate copper coordination, as previously reported (*29*). As the pH increases further, the copper is able to compete with protons for glycine amides, and hence, four coppers are able to bind in the classic single-copper to single-histidine coordination, with contributions from the deprotonated amides from the adjacent glycine residues. This multistage coordination is clearly also occurring in the octarepeat region at physiological pH, but driven by copper concentration as opposed to competition from protons. Using a sequential binding model, a clear negative cooperativity in copper binding can be seen as the copper concentration increases. At copper equivalents of less than one, a high-affinity binding site is immediately obvious, involving the four-histidine complex. As the copper concentration increases further, a binding event that is 4 orders of magnitude weaker is apparent, with two further sites of slightly higher affinity. It is likely that the sequential affinity for copper at this second binding site is adversely affected by the disruption of three imidazole bonds as the coordination mode changes. Again, in the presence of the other region, the octarepeat appears to suffer a slight reduction in the affinity for copper within its high-affinity site. There can be no doubt that this remarkable ability to alter coordination and hence structure at different copper concentrations will be highly significant to the function of the protein and, combined with previous studies indicating a copper concentration-dependent uptake and internalization (*10, 12*), supports a potential role in copper sensing, sequestration, and internalization within the synaptic cleft. This ability would be highly dependent on copper binding to the octarepeat region. Any such function would have an important role in reducing the toxic effects from copper within the brain.

One important aspect of this study has been the determination of the binding affinities for copper on native PrP. Our data clearly show that the number of sites and their affinity for copper are similar to those of the recombinant protein. This therefore confirms that in vivo alterations to the protein such as glycosylation do not affect the copper binding capabilities. It is also confirmation that metal binding studies on full-length recombinant protein are a reasonable model for that of the native protein. As many previous studies which have shown dramatically different findings are based on peptide fragments (*25, 26*), this work should now finally put to rest the differences in opinion over the affinity of copper for PrP.

Studies on the binding of other metals with PrP are largely in agreement with the published pattern of cation binding to amino acids (*50*). These data suggest that the affinity of amino acid residues with metals follows the pattern of alkali metals < earth metals < transition metals. There is no apparent binding of Mg to PrP, but all of the transition metals tested do produce isothermal data. As with copper, this binding is dependent on pH. Ni and Zn both bind with the highest affinity to the octarepeat region and at pH 7, whereas Fe binds with highest affinity at the fifth site. Under acidic conditions, only Fe is able to bind and at the fifth site. This is again further evidence of two very different binding mechanisms within the octarepeat and the fifth site. Divalent cations which are able to bind the fifth site appear to do so under acidic or neutral conditions, whereas binding within the octarepeat is always optimal under neutral to mildly basic conditions. This would suggest the involvement of histidines for the binding of other metals as well as copper. Even under optimal conditions, it would seem unlikely that the associations of these metals with PrP play a role in its physiological function due to their relatively low stability constants from PrP. When they are compared to those of physiological systems associated with these metals, it is clear that such low affinity values would be unlikely to enable PrP to have a role in transport, storage, or catalysis in connection with Fe, Ni, or Zn. For example, transferrin has been shown to bind Fe with an affinity of 10^{23} (*51*) and Cu/Zn SOD binds Zn with an affinity of 4.2×10^{14} (*52*). It is also clear that, under physiological conditions, these metals would be unable to displace copper from the protein even in a free ionic form.

One of the most heated topics of debate concerning the prion protein's function is whether it is able to act in an antioxidant role. Much recent evidence has been contradictory, with studies confirming antioxidant activity (*5, 15*−*18*) and other studies showing this not to be so (*19, 20*). The need to develop a technique that can be built on to contribute to this argument is therefore desirable. We have applied a new technique to the study of metal binding to PrP which may aid further a solution to this question. Although previous electrochemical work exists on small peptide fragments analogous to single octarepeat copper binding regions (*45, 46*), no study has used the entire protein stably adsorbed to the electrode surface. By adsorbing PrP to a diamond electrode and subjecting it to cyclic voltammetry, we have shown without doubt that the protein is capable of exchanging electrons when bound to copper. This electrochemistry is largely dependent on the copper bound to the octarepeat region but also involves the fifth site, but not independently. This appears to be further evidence for the interaction between the two copper binding regions. The redox cycling is limited by the rate of electron transfer and is fully reversible, indicating that the protein is unaffected by continuous oxidation and reduction. Despite the proposed

square planner copper coordination geometry, copper(I) and copper(II) are able to remain stably bound to the protein during cycling. Previous work has demonstrated this property (*45*). The calculated area taken up on the electrode by the protein, assuming five redox active coppers bound to each, gives a very realistic value of 4.7 nm^2, and experiments with various mutants lacking one or more coppers further prove the results. The midpoint potential of 0.03 mV would mean in vivo conditions would favor a redox able state. Configurational and structural effects due to the adsorption onto the electrode are currently not clearly identified, and further studies on the pH effect and environmental conditions affecting the redox reactivity are in progress. With the enormous body of evidence supporting the importance of oxidative stress in prion disease (*53*) and the evidence supporting PrP as an antioxidant, this new evidence strongly supports the idea that PrP contributes to both the normal defense against oxidative stress and its cause in prion disease (*21, 22*).

REFERENCES

1. Prusiner, S. B. (1998) Prions. *Proc. Natl. Acad. Sci. U.S.A. 95* (23), 13363–13383.
2. Hope, J., Reekie, L. J., Hunter, N., Multhaup, G., Beyreuther, K., White, H., Scott, A. C., Stack, M. J., Dawson, M., and Wells, G. A. (1988) Fibrils from brains of cows with new cattle disease contain scrapie-associated protein. *Nature 336* (6197), 390–392.
3. Hsiao, K., and Prusiner, S. B. (1990) Inherited human prion diseases. *Neurology 40* (12), 1820–1827.
4. Bueler, H., Aguzzi, A., Sailer, A., Greiner, R. A., Autenried, P., Aguet, M., and Weissmann, C. (1993) Mice devoid of PrP are resistant to scrapie. *Cell 73* (7), 1339–1347.
5. Brown, D. R., Clive, C., and Haswell, S. J. (2001) Antioxidant activity related to copper binding of native prion protein. *J. Neurochem. 76* (1), 69–76.
6. Mouillet-Richard, S., Ermonval, M., Chebassier, C., Laplanche, J. L., Lehmann, S., Launay, J. M., and Kellermann, O. (2000) Signal transduction through prion protein. *Science 289* (5486), 1925–1928.
7. Schmitt-Ulms, G., Legname, G., Baldwin, M. A., Ball, H. L., Bradon, N., Bosque, P. J., Crossin, K. L., Edelman, G. M., DeArmond, S. J., Cohen, F. E., and Prusiner, S. B. (2001) Binding of neural cell adhesion molecules (N-CAMs) to the cellular prion protein. *J. Mol. Biol. 314* (5), 1209–1225.
8. Mange, A., Milhavet, O., Umlauf, D., Harris, D., and Lehmann, S. (2002) PrP-dependent cell adhesion in N2a neuroblastoma cells. *FEBS Lett. 514* (2−3), 159–162.
9. Santuccione, A., Sytnyk, V., Leshchyns'ka, I., and Schachner, M. (2005) Prion protein recruits its neuronal receptor NCAM to lipid rafts to activate p59fyn and to enhance neurite outgrowth. *J. Cell Biol. 169* (2), 341–354.
10. Pauly, P. C., and Harris, D. A. (1998) Copper stimulates endocytosis of the prion protein. *J. Biol. Chem. 273* (50), 33107–33110.
11. Brown, D. R. (1999) Prion protein expression aids cellular uptake and veratridine-induced release of copper. *J. Neurosci. Res. 58* (5), 717–725.
12. Haigh, C. L., Edwards, K., and Brown, D. R. (2005) Copper binding is the governing determinant of prion protein turnover. *Mol. Cell. Neurosci. 30* (2), 186–196.
13. Kuwahara, C., Takeuchi, A. M., Nishimura, T., Haraguchi, K., Kubosaki, A., Matsumoto, Y., Saeki, K., Matsumoto, Y., Yokoyama, T., Itohara, S., and Onodera, T. (1999) Prions prevent neuronal cell-line death. *Nature 400* (6741), 225–226.
14. Roucou, X., Gains, M., and LeBlanc, A. C. (2004) Neuroprotective functions of prion protein. *J. Neurosci. Res. 75* (2), 153–161.
15. Brown, D. R., Wong, B. S., Hafiz, F., Clive, C., Haswell, S. J., and Jones, I. M. (1999) Normal prion protein has an activity like that of superoxide dismutase. *Biochem. J. 344* (Part 1), 1–5.
16. Wong, B. S., Chen, S. G., Colucci, M., Xie, Z., Pan, T., Liu, T., Li, R., Gambetti, P., Sy, M. S., and Brown, D. R. (2001) Aberrant metal binding by prion protein in human prion disease. *J. Neurochem. 78* (6), 1400–1408.
17. Thackray, A. M., Knight, R., Haswell, S. J., Bujdoso, R., and Brown, D. R. (2002) Metal imbalance and compromised antioxidant function are early changes in prion disease. *Biochem. J. 362* (Part 1), 253–258.
18. Cui, T., Daniels, M., Wong, B. S., Li, R., Sy, M. S., Sassoon, J., and Brown, D. R. (2003) Mapping the functional domain of the prion protein. *Eur. J. Biochem. 270* (16), 3368–3376.
19. Hutter, G., Heppner, F. L., and Aguzzi, A. (2003) No superoxide dismutase activity of cellular prion protein in vivo. *Biol. Chem. 384* (9), 1279–1285.
20. Jones, S., Batchelor, M., Bhelt, D., Clarke, A. R., Collinge, J., and Jackson, G. S. (2005) Recombinant prion protein does not possess SOD-1 activity. *Biochem. J. 392* (Part 2), 309–312.
21. Stanczak, P., and Kozlowski, H. (2007) Can chicken and human PrPs possess SOD-like activity after β-cleavage? *Biochem. Biophys. Res. Commun. 352* (1), 198–202.
22. Treiber, C., Pipkorn, R., Weise, C., Holland, G., and Multhaup, G. (2007) Copper is required for prion protein-associated superoxide dismutase-I activity in *Pichia pastoris*. *FEBS J. 274* (5), 1304–1311.
23. Brown, D. R., Qin, K., Herms, J. W., Madlung, A., Manson, J., Strome, R., Fraser, P. E., Kruck, T., von Bohlen, A., Schulz-Schaeffer, W., Giese, A., Westaway, D., and Kretzschmar, H. (1997) The cellular prion protein binds copper in vivo. *Nature 390* (6661), 684–687.
24. Thompsett, A. R., Abdelraheim, S. R., Daniels, M., and Brown, D. R. (2005) High affinity binding between copper and full-length prion protein identified by two different techniques. *J. Biol. Chem. 280* (52), 42750–42758.
25. Hornshaw, M. P., McDermott, J. R., Candy, J. M., and Lakey, J. H. (1995) Copper binding to the N-terminal tandem repeat region of mammalian and avian prion protein: Structural studies using synthetic peptides. *Biochem. Biophys. Res. Commun. 214* (3), 993–999.
26. Jackson, G. S., Murray, I., Hosszu, L. L., Gibbs, N., Waltho, J. P., Clarke, A. R., and Collinge, J. (2001) Location and properties of metal-binding sites on the human prion protein. *Proc. Natl. Acad. Sci. U.S.A. 98* (15), 8531–8535.
27. Stanczak, P., Valensin, D., Juszczyk, P., Grzonka, Z., Migliorini, C., Molteni, E., Valensin, G., Gaggelli, E., and Kozlowski, H. (2005) Structure and stability of the CuII complexes with tandem repeats of the chicken prion. *Biochemistry 44* (39), 12940–12954.
28. Chattopadhyay, M., Walter, E. D., Newell, D. J., Jackson, P. J., Aronoff-Spencer, E., Peisach, J., Gerfen, G. J., Bennett, B., Antholine, W. E., and Millhauser, G. L. (2005) The octarepeat domain of the prion protein binds Cu(II) with three distinct coordination modes at pH 7.4. *J. Am. Chem. Soc. 127* (36), 12647–12656.
29. Wells, M. A., Jelinska, C., Hosszu, L. L., Craven, C. J., Clarke, A. R., Collinge, J., Waltho, J. P., and Jackson, G. S. (2006) Multiple forms of copper (II) co-ordination occur throughout the disordered N-terminal region of the prion protein at pH 7.4. *Biochem. J. 400* (3), 501–510.
30. Garnett, A. P., and Viles, J. H. (2003) Copper binding to the octarepeats of the prion protein. Affinity, specificity, folding, and cooperativity: Insights from circular dichroism. *J. Biol. Chem. 278* (9), 6795–6802.
31. Morante, S., Gonzalez-Iglesias, R., Potrich, C., Meneghini, C., Meyer-Klaucke, W., Menestrina, G., and Gasset, M. (2004) Inter- and intra-octarepeat Cu(II) site geometries in the prion protein: Implications in Cu(II) binding cooperativity and Cu(II)-mediated assemblies. *J. Biol. Chem. 279* (12), 11753–11759.
32. Walter, E. D., Chattopadhyay, M., and Millhauser, G. L. (2006) The affinity of copper binding to the prion protein octarepeat domain: Evidence for negative cooperativity. *Biochemistry 45* (43), 13083–13092.
33. Miura, T., Hori-i, A., and Takeuchi, H. (1996) Metal-dependent α helix formation promoted by the glycine-rich octapeptide region of prion protein. *FEBS Lett. 396* (2−3), 248–252.
34. Tsenkova, R. N., Iordanova, I. K., Toyoda, K., and Brown, D. R. (2004) Prion protein fate governed by metal binding. *Biochem. Biophys. Res. Commun. 325* (3), 1005–1012.
35. Viles, J. H., Cohen, F. E., Prusiner, S. B., Goodin, D. B., Wright, P. E., and Dyson, H. J. (1999) Copper binding to the prion protein: Structural implications of four identical cooperative binding sites. *Proc. Natl. Acad. Sci. U.S.A. 96* (5), 2042–2047.
36. Daniels, M., and Brown, D. R. (2002) Purification and preparation of prion protein: Synaptic superoxide dismutase. *Methods Enzymol. 349*, 258–267.

37. Wiseman, T., Williston, S., Brandts, J. F., and Lin, L. N. (1989) Rapid measurement of binding constants and heats of binding using a new titration calorimeter. *Anal. Biochem. 179* (1), 131–137.
38. Sigurskjold, B. W. (2000) Exact analysis of competition ligand binding by displacement isothermal titration calorimetry. *Anal. Biochem. 277* (2), 260–266.
39. Martell, A. E., and Smith, R. M. (1974) *Critical Stability Constants*, Plenum Press, New York.
40. Zhang, Y., Akilesh, S., and Wilcox, D. E. (2000) Isothermal titration calorimetry measurements of Ni(II) and Cu(II) binding to His, GlyGlyHis, HisGlyHis, and bovine serum albumin: A critical evaluation. *Inorg. Chem. 39* (14), 3057–3064.
41. Davies, P., and Brown, D. R. (2009) A Critical Assessment of Two Methods of Mathematical Analysis for Complex Protein and Chelated Ligand Thermodynamics. *Dalton Trans.* .
42. Millhauser, G. L. (2004) Copper binding in the prion protein. *Acc. Chem. Res. 37* (2), 79–85.
43. Johnson, C. J., Phillips, K. E., Schramm, P. T., McKenzie, D., Aiken, J. M., and Pedersen, J. A. (2006) Prions adhere to soil minerals and remain infectious. *PLoS Pathog. 2* (4), e32.
44. Bard, A. J., and Faulkner, L. R. (2001) *Electrochemical methods: Fundamentals and applications*, 2nd ed., p xxi, John Wiley, New York.
45. Hureau, C., Charlet, L., Dorlet, P., Gonnet, F., Spadini, L., Anxolabehere-Mallart, E., and Girerd, J. J. (2006) A spectroscopic and voltammetric study of the pH-dependent Cu(II) coordination to the peptide GGGTH: Relevance to the fifth Cu(II) site in the prion protein. *J. Biol. Inorg. Chem. 11* (6), 735–744.
46. Hureau, C., Mathe, C., Faller, P., Mattioli, T. A., and Dorlet, P. (2008) Folding of the prion peptide GGGTHSQW around the copper(II) ion: Identifying the oxygen donor ligand at neutral pH and probing the proximity of the tryptophan residue to the copper ion. *J. Biol. Inorg. Chem. 13* (7), 1055–1064.
47. Hornshaw, M. P., McDermott, J. R., and Candy, J. M. (1995) Copper binding to the N-terminal tandem repeat regions of mammalian and avian prion protein. *Biochem. Biophys. Res. Commun. 207* (2), 621–629.
48. Millhauser, G. L. (2007) Copper and the prion protein: Methods, structures, function, and disease. *Annu. Rev. Phys. Chem. 58*, 299–320.
49. Jones, C. E., Abdelraheim, S. R., Brown, D. R., and Viles, J. H. (2004) Preferential Cu^{2+} coordination by His96 and His111 induces β-sheet formation in the unstructured amyloidogenic region of the prion protein. *J. Biol. Chem. 279* (31), 32018–32027.
50. Gilli, R., Lafitte, D., Lopez, C., Kilhoffer, M., Makarov, A., Briand, C., and Haiech, J. (1998) Thermodynamic analysis of calcium and magnesium binding to calmodulin. *Biochemistry 37* (16), 5450–5456.
51. Aisen, P., Leibman, A., and Pinkowitz, R. A. (1974) The anion-binding functions of transferrin. *Adv. Exp. Med. Biol. 48*, 125–140.
52. Crow, J. P., Sampson, J. B., Zhuang, Y., Thompson, J. A., and Beckman, J. S. (1997) Decreased zinc affinity of amyotrophic lateral sclerosis-associated superoxide dismutase mutants leads to enhanced catalysis of tyrosine nitration by peroxynitrite. *J. Neurochem. 69* (5), 1936–1944.
53. Brown, D. R. (2005) Neurodegeneration and oxidative stress: Prion disease results from loss of antioxidant defence. *Folia Neuropathol. 43* (4), 229–243.

BI900170N